Dalton Transactions

Accepted Manuscript

ROYAL SOCIETY OF CHEMISTRY

rsc.li/dalton

View Article Online
DOI: 10.1039/C6DT02969H

Synopsis:

A series of water soluble ruthenium arene RAPTA like compounds have been prepared One of the four compounds with a novel valence tautomerized ancillary ligand shows marked antiproliferarive and thiredoxin reductase inhibition property .

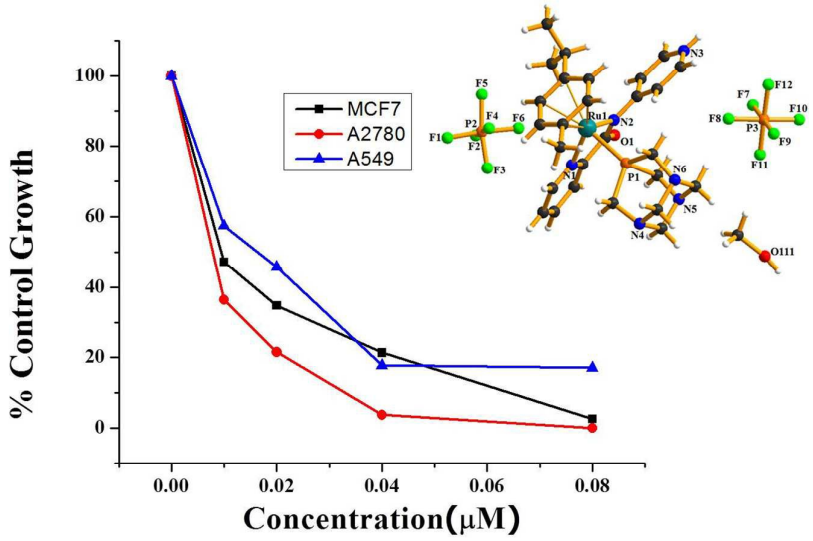

Fine tuning through valence bond tautomerization of ancillary ligand in ruthenium(II) arene complex for better anticancer activity and enzyme inhibition property

Poulami Mandal,[a] Novina Malviya,[a] M. Fátima C. Guedes da Silva,[b] Sandeep Singh Dhankhar,[c] C. M. Nagaraja,[c] Shaikh M Mobin, [a,d] Suman Mukhopadhyay[*, a,d]

[a] *Department of Chemistry, School of Basic Sciences, Indian Institute of Technology Indore, Indore 453552, India.*

[b] *Centro de Química Estrutural, Complexo I, Instituto Superior Técnico, Technical University of Lisbon, Avenida Rovisco Pais,1049-001, Lisbon, Portugal*

[c] *Department of Chemistry, Indian Institute of Technology Ropar, Rupnagar 140001, Punjab, India*

[d] *Centre for Bioscience and Biomedical Engineering (BSBE), Indian Institute of Technology Indore, Indore 453552, India.*

Tel : +91 731 2438 735 Fax: +91 731 2361 482

E-mail: suman@iiti.ac.in

Introduction:

Arene ruthenium (II) complexes with pseudo-octahedral coordination environment also named as piano-stool compounds have been studied in recent past widely for its probable application in catalysis, crystal engineering and metallo-pharmaceuticals.[1,2,3,4,5] However because of the their lower toxicity, amphiphilic properties generated from hydrophobic arene ring and hydrophilic metal center, improved selectivity and possibility to play around with the ligands to improve the target (DNA, enzyme and proteins) specific chemotherapy make them an important class of compounds with biological significance. Ruthenium arene complexes have shown significant antimetastatic and anticancer properties which can be modulated by factors like hydrophobicity of arene ligand and hydrogen bond forming ability and other properties of the ancillary ligands.[6,7,8] One of the biggest advantage of ruthenium complexes is that they are transported inside cancer cells by transferrin enzyme, an iron transporter in human body which promotes selective accumulation of ruthenium compound in cancer cells which overexpress the transferring receptor.[9] The problem of water solubility of

View Article Online
DOI: 10.1039/C6DT02969H

the ruthenium-arene complexes has been largely tackled by introduction of amphiphilic ligand called PTA (PTA = 1,3,5-triaza-7-phospha-tricyclo-[3.3.1.1]decane) to generate a ruthenium-arene-PTA combination known as RAPTA compounds.[10,11,12,13] With fixation of arene ring and PTA ligand coordinated to ruthenium center, scientists around the world have tried different ancillary ligands with various characteristics to evaluate possible effect on cytotoxicity and target specificity.[14,15,16,17] Recently some reports have been published where picolinamide or carboxamide complexes have shown interesting anticancer properties due to their dynamic coordinating nature to the metal center. [18,19,20,21] To explore the reactivity of picolinamide based ligands we have utilized nitro substituted aniline and 3-pyridyl and 4-pyridyl amine to generate picolinamide derivatives to monitor the effect of ancillary ligands on anticancer activity as to the best of our knowledge there is no report where N-substituted picolinamide part as ancillary ligand is modulated in RAPTA scaffold to explore the anticancer properties of the synthesized complexes. Interestingly one of the synthesized compound has shown marked antiproliferative activity against different cancer cell lines. As it is evident that RAPTA compounds work upon molecular targets other than DNA,[22] we have explored the interaction of the synthesized complexes with thioredoxin reductase (TrxR) which is one of the key target identified[23] previously because of the presence of selenolate group which after reduction prefers to bind with softer metal ion making it suitable as a pharmacological target suitable for metallodrugs.

Experimental section

Materials and Methods

All the chemical reagents required were purchased from Sigma and used without further purification. NMR spectra were recorded on an AVANCE III 400 Ascend Bruker BioSpin machine at ambient temperature. Mass spectrometric analyses were done on Bruker-Daltonics, microTOF-Q II mass spectrometer and elemental analyses were carried out with a ThermoFlash 2000 elemental analyzer. Spectrophotometric measurements were performed on a Varian UV-Vis spectrophotometer (Model: Cary 100) (for absorption) and a Fluoromax-4p spectrofluorometer from Horiba JobinYvon (Model: FM-100) (for emission) using a quartz cuvette with path length of 1 cm. Far-ultraviolet (UV) (190 to 260 nm) spectra were recorded in 0.1 cm path length cell (Hellma, Muellheim/Baden, Germany) using a step size of 0.5 nm, bandwidth of 1 nm and a scan rate of 20 nm min^{-1}. Conductivity measurements were done using a Digital Conductivity Meter Model 611 instrument. Conductivities of complexes were

obtained with 1 mM solutions in acetonitrile. [Ru(L^1)(η^6-p-cymene)Cl] **1** and [Ru(L^1)(η^6-benzene)Cl] **3** [HL^1 = pyridine-2-carboxylic acid (4-nitro-phenyl)amide] were prepared by literature method.[24] Ligand HL^2 [HL^2 = 4-(N-(2-Pyridyl)carbamoyl pyridine] and HL^3 [HL^3 = 3-(N-(2-Pyridyl)carbamoyl) pyridine], were also prepared by method reported earlier.[25] The sulforhodamine B (SRB) growth inhibition (GI_{50}) assays were carried out by Advanced Center for Treatment, Research and Education in Cancer (ACTREC), Mumbai by following the literature procedure.[26]

[RuL^1(η^6-p-cymene)PTA][BF_4] 2 . 2H_2O

0.05g (0.09 mmol) of compound [RuL^1(η^6-p-cymene)Cl] **1** was dissolved in 20 mL of methanol. A methanolic solution (10 mL) of 1,3,5-triaza-7-phosphoadamantane (PTA) (0.01g, 0.09 mmol) was added dropwise to the solution of compound **1**. The reaction mixture was stirred for 2 h at room temperature and then filtered. The filtrate was reduced in vacuo to a volume of *ca.* 5 mL. An excess of diethyl ether was added to accomplish precipitation. The precipitate was filtered, washed with diethyl ether and dried in *vacuo* to afford yellow coloured crystalline solid as product. Yield: 76%. The yellow coloured compound was dissolved in methanol. A methanolic soln of $NaBF_4$ (0.1 g, 0.08 mmol) was added to it and stirred for 2 h. The resulting solution was then filtered and filtrate was then concentrated in *vacuo* to a volume of *ca*.5 mL. The filtrate was kept in refrigerator for overnight, from which crystals suitable for X-ray analysis were obtained. Yield: 62%. ^{1}H NMR (400.13MHz, 298K ,d6-DMSO): δ 8.98 [d, 1H , ^{3}J (^{1}H - ^{1}H) = 4.0 Hz, CH of C_5H_4N], 8.29 [m, 3H, 1XCH of C_5H_4N and 2XCH of $C_6H_4NO_2$], 8.10 [d, 1H, ^{3}J (^{1}H - ^{1}H) = 8.0 Hz, CH of C_5H_4N], 7.84 [t, 1H , ^{3}J (^{1}H - ^{1}H) = 12.0 Hz, CH of C_5H_4N], 7.57 [d, 2H , ^{3}J (^{1}H - ^{1}H) = 12.0 Hz, CH of $C_6H_4NO_2$], 6.26 [d,1H, ^{3}J (^{1}H - ^{1}H) = 4.0 Hz, CH of C_6H_4], 5.92 [d,1H, ^{3}J (^{1}H - ^{1}H)=8.0Hz, CH of C_6H_4], 5.75 [d, 1H , ^{3}J (^{1}H - ^{1}H)=8.0Hz CH of C_6H_4], 5.43[d, 1H, ^{3}J (^{1}H - ^{1}H)=8.0Hz CH of C_6H_4] , 4.37 [m.6H,3xNCH_2N], 4.00 [m ,6H, 3xPCH_2N], 2.84 [m, 1H, CH(CH_3)$_2$], 2.28 [s, 3H, $C_6H_4CH_3$], 0.98 [d, 3H, CH(CH_3)$_2$], 0.74 [d, 3H, CH(CH_3)$_2$] (Fig. S1). ^{13}C NMR (100.61MHz, d6-DMSO): δ 167.0 [C of *C*ON], 157.7 [C of $C_6H_4NO_2$], 156.3 [C of C_5H_4N], 154.1 [CH of C_5H_4N], 142.3 [CH of C_5H_4N], 140.7 [C of $C_6H_4NO_2$], 128.9 [CH of C_5H_4N], 127.1 [2xCH of $C_6H_4NO_2$], 126.7 [CH of C_5H_4N], 124.1 [2xCH of $C_6H_4NO_2$], 119.1 [C of C_6H_4], 101.1 [C of C_6H_4], 91.4 [CH of C_6H_4], 90.1 [CH of C_6H_4], 88.0 [CH of C_6H_4], 87.4 [CH of C_6H_4], 71.4 [3xN*C*H_2N of PTA], 50.0-48.5 [3xP*C*H_2N of PTA], 30.4 [$C_6H_4CH_3$], 21.9 [CH(*C*H_3)$_2$], 20.9 [CH(*C*H_3)$_2$], 18.1 [CH of *C*H(CH_3)$_2$] (Fig. S2). ^{31}P NMR (d6-DMSO, 126 MHz) : δ - 34.4 (Fig. S3). ESI-MS (+ve mode) : [RuL^1(η^6-p-cymene)PTA]$^+$: 635.16

View Article Online
DOI: 10.1039/C6DT02969H

(m/z) (Fig. S4). Anal. Calcd for C28H38BF4N6O5PRu: C, 44.40; H, 5.06; N, 11.09. Found: C, 44.53; H, 5.11; N, 10.89.

[RuL^1(η^6-benzene)PTA][PF$_6$] 4 .CH$_3$OH

Compound [RuL^1(η^6-benzene)Cl] **3** (0.08g, 0.1 mmol) was dissolved in a mixture of methanol (15 mL) and dichloromethane (15 mL). A methanolic solution (10 mL) of 1,3,5-triaza-7-phosphoadamantane (PTA) (0.02g, 0.1 mmol) was added dropwise to the solution of compound **3**. The reaction mixture was stirred for 2 h at room temperature and then filtered. The filtrate was reduced in vacuo to a volume of *ca*. 5 mL. An excess of diethyl ether was added to accomplish precipitation. The precipitate was filtered, washed with diethyl ether and dried in vacuo, affording a yellow solid. Yield: 62%. The yellow coloured compound was dissolved in methanol. A methanolic solution of NH_4PF_6 (0.12 g, 0.1 mmol) was added to it and stirred for 2 h. The resulting solution was then filtered and it was concentrated in vacuo to a volume of *ca*.5 mL.The filtrate was kept for vapour diffusion with diethyl ether, from which crystals suitable for X-ray analysis were obtained. Yield: 52%. ^{1}H NMR(400.13MHz, 298K, d6-DMSO): δ 8.92 [d, 1H , ^{3}J (^{1}H - ^{1}H) = 4.0 Hz CH of C$_5$*H*$_4$N], 8.27-8.24 [m, 2H ,2xCH of C$_6$*H*$_4$NO$_2$], 8.10 [d, 1H , ^{3}J (^{1}H - ^{1}H) = 8.0 Hz, CH of C$_5$*H*$_4$N], 7.93 [br.s,1H,CH of C$_5$*H*$_4$N], 7.76 [t.1H, ^{3}J (^{1}H - ^{1}H) = 12.0 Hz C$_5$*H*$_4$N], 7.54 [d, 2H, ^{3}J (^{1}H - ^{1}H) = 12.0 Hz, 2xCH of C$_6$*H*$_4$NO$_2$], 6.00 [s, 6H ,6xCH of C$_6$*H*$_6$], 4.37 [m, 6H ,3xNC*H*$_2$N of PTA], 3.98 [s, 6H ,3xPC*H*$_2$N of PTA] (Fig. S5). ^{13}C NMR (100.61MHz, d6-DMSO): δ 169.9 [C of *C*ON], 158.8 [C of *C*$_5$H$_4$N], 155.9 [CH of *C*$_5$H$_4$N], 154.6 [C of *C*$_6$H$_4$NO$_2$], 143.9 [C of *C*$_6$H$_4$NO$_2$], 139.2 [CH of *C*$_5$H$_4$N], 129.4 [CH of *C*$_5$H$_4$N], 127.8 [2xCH of *C*$_6$H$_4$NO$_2$], 127.2 [CH of *C*$_5$H$_4$N], 124.2 [2xCH of *C*$_6$H$_4$NO$_2$], 85.9 [6xCH of *C*$_6$H$_6$], 72.5 [3xNC*H*$_2$N of PTA], 52.2 [3xPC*H*$_2$N of PTA] (Fig. S6). ^{31}P NMR (126 MHz, d6-DMSO): δ -39.16[s, PTA], -144.1[sept, *P*F$_6$] (Fig. S7). ESI-MS (+ve mode) : [RuL^1(η^6-benzene)PTA]$^+$: 579.1(m/z) (Fig. S8). Anal. Calcd for C25H30F6N6O4P2Ru: C, 39.74; H, 4.00; N, 11.12. Found: C, 39.56; H, 4.32; N, 10.89.

[RuL^2(η^6-p-cymene)Cl] 5

0.05g of [(η^6-p-cymene)RuCl(*μ*-Cl)]$_2$ (0.08 mmol) was dissolved in 20 mL of dichloromethane and the ligand (HL^2) [4-(N-(2-Pyridyl)carbamoyl pyridine] (0.32g, 0.16mmol), dissolved in methanol was added dropwise. The mixture was stirred at room temperature for 4 h . The resulting solution was then filtered and evaporated in vacuo to *ca*.5

mL. Addition of excess diethyl ether to the filtrate leads to the formation of orange coloured precipitate. The precipitate was filtered, washed with hexane and dried in open air affording the title compound as orange solid. Yield 54%. ^{1}H NMR (400.13MHz, 298K, $CDCl_3$): δ 9.03 [br s, 1H , CH of C_5H_4N of 4-amino pyridine], 8.37 [broad, 2H ,CH of C_5H_4N of 4-amino pyridine], 8.05 [d, 1H , CH of C_5H_4N of picolinic acid], 7.97 [t, 1H, CH of C_5H_4N of picolinic acid], 7.58 [t, 1H, CH of C_5H_4N of picolinic acid], 6.81 [d, 2H ,CH of C_5H_4N of 4-amino pyridine], 5.49 [d, 1H, ,CH of C_6H_4], 5.32 [d, 2H, , CH of C_6H_4], 5.28 [d, 1H, , CH of C_6H_4], 2.46 [sept, 1H, $CH(CH_3)_2$], 2.23 [s, 3H, $C_6H_4CH_3$], 1.05 [d, 3H, $CH(CH_3)_2$], 0.99 [d, 3H, $CH(CH_3)_2$] (Fig. S9). ESI-MS (+ve mode) : $[RuL^2(\eta^6\text{-p-cymene})]^+$: 434.1 (m/z) (Fig. S10).

$[Ru(HL^2)(\eta^6\text{-p-cymene})PTA][PF_6]_2$ 6 .CH_3OH

A 10 mL methanolic solution of 1,3,5-triaza-7-phosphoadamantane (0.35g, 0.22 mmol) was added dropwise to a solution of compound **5** (0.1g, 0.22mmol) dissolved in a mixture of methanol and dichloromethane (10mL + 10mL). The resulting solution was then stirred overnight at room temperature and filtered. The filtrate was then evaporated to dryness to get the crude product as yellow solid. Yield: 78%. The obtained compound was then dissolved in methanol (0.5 g, 0.08 mmol) and a methanolic solution of NH_4PF_6 (0.03 g, 0.18 mmol) was then added to it .The resulting solution was allowed to stir for 2h at room temperature. The mixture was then filtered and concentrated to 5 mL and kept at 0°C for overnight. Yellow coloured crystals suitable for single crystal XRD was obtained from the reaction mixture. Yield: 70%. ^{1}H NMR (400.13MHz, 298K ,d6-DMSO) : δ 9.00 [d, 1H , ^{3}J (^{1}H - ^{1}H) = 4.0 Hz, CH of C_5H_4N], 8.64 [d, 2H, 2xCH of substituted 4-amino pyridine], 8.36 [t, 1H , ^{3}J (^{1}H - ^{1}H) = 12.0 Hz, CH of C_5H_4N], 8.21 [d, 1H , ^{3}J (^{1}H - ^{1}H) = 4.0 Hz, CH of C_5H_4N], 7.92 [d,1H, ^{3}J (^{1}H - ^{1}H) = 8.0 Hz, CH of C_5H_4N], 7.87 [d,2H, ^{3}J (^{1}H - ^{1}H)=8.0Hz, 2xCH of substituted 4-amino pyridine], 6.29 [d, 1H , ^{3}J (^{1}H - ^{1}H)=4.0Hz CH of C_6H_4], 6.06[d, 1H, CH of C_6H_4] , 5.87[d, 1H, CH of C_6H_4] ,5.78[d, 1H, CH of C_6H_4] , 4.41 [m, 6H,3xNCH_2N], 3.99 [m, 6H, 3xPCH_2N], 2.43 [s,3H, $C_6H_4CH_3$], 2.26 [sept, 1H, CH of $CH(CH_3)_2$],0.99 [d, 3H, $CH(CH_3)_2$], 0.73[d,3H,$CH(CH_3)_2$] (Fig. S11). ^{13}C NMR (100.61MHz, d6-DMSO) : δ 168.6 [C of CON] , 156.7 [C of substitued 4-amino pyridine], 153.0 [2xCH of substituted 4-amino pyridine] , 142.5 [CH of C_5H_4N], 141.0 [CH of C_5H_4N], 129.8 [CH of C_5H_4N], 127.5 [CH of C_5H_4N], 122.4 [CH of substitued 4-amino pyridine], 121.0 [CH of substitued 4-amino pyridine],101.6 [C of C_6H_4], 90.9 [C of C_6H_4], 87.9 [2xCH of C_6H_4], 78.5 [2xCH of C_6H_4], 71.2 [3xNCH_2N of PTA], 49.9-48.5 [3xPCH_2N of PTA], 30.6 [$C_6H_4CH_3$], 21.9 [$CH(CH_3)_2$], 20.9 [$CH(CH_3)_2$],

18.4 [CH of *C*H(*C*H$_3$)$_2$] (Fig. S12). ^{31}P NMR (d6-DMSO, 126 MHz) : δ -38.9, -144.2 [sept, *P*F$_6$] (Fig. S13). ESI-MS (+ve mode) : 296.1(m/z) :[RuL^2(η^6-p-cymene)]$^{2+}$/2 (Fig. S14).Anal. Calcd for C28H39F12N6O2P3Ru: C, 36.81; H, 4.30; N, 9.20. Found: C, 36.90; H, 4.54; N, 9.45

[RuL^3(η^6-p-cymene)Cl] 7

0.1g of [(η^6-p-cymene)RuCl(*μ*-Cl)]$_2$ (0.16mmol) was dissolved in 50 mL of methanol and methanolic solution of ligand (HL^3) [3-(N-(2-Pyridyl)carbamoyl) pyridine] (0.65g, 0.32mmol) was added dropwise to that. The mixture was stirred at room temperature for 4 h . The resulting solution was then filtered. The filtrate was evaporated in vacuo of ca.5 mL. An excess of diethyl ether was added to accomplish precipitation. The precipitate was filtered, washed with hexane and dried in open air affording the title compound as orange solid. Yield 42%. ^{1}H NMR(400.13MHz, 298K, CDCl$_3$): δ 9.54 [s, 1H CH of substituted 3-amino pyridine], 9.02 [s, 1H ,CH of C$_5$*H*$_4$N], 8.76 [d, 1H , CH of C$_5$*H*$_4$N], 8.36 [d, 1H, CH of substituted 3-amino pyridine], 8.12 [d, 1H, CH of substituted 3-amino pyridine], 7.96 [t , 1H , CH of C$_5$*H*$_4$N], 7.54 [t, 1H ,CH of C$_5$*H*$_4$N], 7.22 [t, 1H ,CH of substituted 3-amino pyridine], 5.65 [d, 1H, ^{3}J (^{1}H - ^{1}H) = 7.8Hz ,CH of C$_6$*H*$_4$], 5.57 [d, 1H, CH of C$_6$*H*$_4$], 5.49 [d, 1H, ^{3}J (^{1}H - ^{1}H) = 7.7Hz, CH of C$_6$*H*$_4$], 5.30 [d, 1H, CH of C$_6$*H*$_4$], 2.85 [sept, 1H, C*H*(CH$_3$)$_2$], 2.26 [s, 3H, C$_6$H$_4$C*H*$_3$], 1.14 [d, 3H, CH(C*H*$_3$)$_2$], 1.05 [d, 3H, CH(C*H*$_3$)$_2$] (Fig. S15) . ESI-MS (+ve mode) : [RuL^3(η^6-p-cymene)]$^+$: 434.0(m/z) (Fig. S16).

[RuL^3(η^6-p-cymene)PTA][BF$_4$] 8

To a solution of compound **7** (0.1 g, 0.22 mmol) dissolved in methanol (20mL), a 10 mL methanolic solution of 1,3,5-triaza-7-phosphoadamantane (0.35g, 0.22mmol) was added dropwise. The resulting mixture was stirred overnight at room temperature and filtered. The filtrate was then evacuated in vacuo to get the crude product as orange coloured solid. Yield: 70%. The orange solid was then dissolved in a mixture of dichloromethane and methanol (5mL+5mL) and a methanolic solution of NaBF$_4$ (0.006g, 0.05mmol) was added to it. The resulting solution was the stirred at room temperature for 2 h and the filtered. The filtrate was then concentrated in vacuo to 2 mL and kept for vapour diffusion with diethyl ether to get orange coloured crystal of compound **8** . Yield: 65%. ^{1}H NMR (400.13MHz, 298K ,d6-DMSO) :δ 8.98 [d, 1H , ^{3}J (^{1}H - ^{1}H) = 4.0 Hz, CH of C$_5$*H*$_4$N], 8.68 [s, 1H, CH of substituted 3-amino pyridine], 8.40 [br.s,1H, CH of C$_5$*H*$_4$N], 8.29 [t, 1H, ^{3}J (^{1}H - ^{1}H) = 12.0 Hz, CH of

substituted 3-amino pyridine], 8.07 [d, 1H , ^{3}J (^{1}H - ^{1}H) = 12.0 Hz, CH of substituted 3-amino pyridine], 7.84 [t, 1H , ^{3}J (^{1}H - ^{1}H) = 4.0 Hz, CH of C_5H_4N], 7.76 [d,1H, ^{3}J (^{1}H - ^{1}H) = 8.0 Hz, CH of C_5H_4N], 7.54 [br.t,1H, ^{3}J (^{1}H - ^{1}H)=8.0 Hz, CH of substituted 3-amino pyridine], 6.29 [d, 1H , ^{3}J (^{1}H - ^{1}H)=4.0Hz CH of C_6H_4], 6.06 [d, 1H, CH of C_6H_4] , 5.87 [d, 1H, CH of C_6H_4] ,5.78 [d, 1H, CH of C_6H_4] , 4.41 [m.6H, 3xNCH_2N], 3.99 [m ,6H, 3xPCH_2N], 2.43 [s, 3H, $C_6H_4CH_3$], 2.26 [sept, 1H, CH of C$H(CH_3)_2$],0.93 [d, 3H, CH(CH_3)$_2$], 0.75[d,3H,CH(CH_3)$_2$] (Fig. S17). ^{13}C NMR (100.61MHz, d6-DMSO) : δ 167.0 [C of *C*ON] , 157.2 [CH of C_5H_4N], 156.3 [CH of C_5H_4N] , 154.2 [C of substituted 3-amino pyridine], 147.5 [C of C_5H_4N substituted 3-amino pyridine], 144.5 [CH of C_5H_4N], 140.6 [CH of substituted 3-amino pyridine], 133.5 [CH of C_5H_4N], 129.3 [CH of C_5H_4N],118.7 [CH of substituted 3-amino pyridine], 115.2 [CH of substituted 3-amino pyridine], 101.8 [C of C_6H_4], 93.5 [C of C_6H_4], 91.3 [CH of C_6H_4], 88.8[CH of C_6H_4], 87.5 [C of C_6H_4], 79.4-70.6 [3xPCH_2N of PTA], 53.7- 46.2 [3xNCH_2N of PTA], 30.2 [$C_6H_4CH_3$], 21.9 [CH(CH_3)$_2$], 21.1 [CH(CH_3)$_2$], 17.9 [CH of C$H(CH_3)_2$] (Fig. S18). ^{31}P NMR (d6-DMSO, 126 MHz) : δ -39.1 (Fig. S19). ESI-MS (+ve mode) : [RuL^3(η^6-p-cymene)PTA]$^+$: 591.15 (m/z) (Fig. S20). Anal. Calcd for C27H34BF4N6OPRu: C, 47.87; H, 5.06; N, 12.41. Found: C, 47.53; H, 5.31; N, 12.47

X-ray crystallography

Compound **2**

X-ray single crystal of complex **2** was immersed in cryo-oil, mounted in Nylon loops and measured at a temperature of 150 K in a Bruker AXS-KAPPA APEX II with graphite monochromated Mo-Kα (λ=0.71073) radiation. Data were collected using omega scans of 0.5º per frame and full sphere of data were obtained. Cell parameters were retrieved using Bruker SMART[27] software and refined using Bruker SAINT[28] on all the observed reflections. Absorption corrections were applied using SADABS.[29] Structures were solved by direct methods by using the SHELXS–97 package[30] and refined with SHELXL–2014/7.[31] Calculations were performed using the WinGX System–Version 2014.1.[32] Least square refinements with anisotropic thermal motion parameters for all the non-hydrogen atoms and isotropic for the remaining atoms

View Article Online
DOI: 10.1039/C6DT02969H

were employed. All hydrogen atoms bonded to carbon were included in the model at geometrically calculated positions and refined using a riding model. Uiso(H) were defined as 1.2Ueq of the parent carbon atoms for phenyl and methylene residues and 1.5Ueq of the parent carbon atoms for the methyl groups. There was some void in the structure which, despite the negligible volume and number of electrons (63 Å3 and 3 electrons per unit cell), was corrected with PLATON/SQUEEZE.[33]

Compound **4**

X-ray single crystal structural data of compound **4** was collected on a Bruker D8 Venture PHOTON 100 CMOS diffractometer equipped with a INCOATEC microfocus source and graphite monochromated Mo Kα radiation (λ = 0.71073 Å) operating at 50 kV and 30 mA. The program SAINT85 was used for integration of diffraction profiles and absorption correction was done with SADABS86 program. The structure was solved by SIR 9287 and refined by full matrix least-square method using SHELXL-201388 and WinGX system, v 2013.3.89. All the nonhydrogen atoms were located from the difference Fourier map and refined anisotropically. All the hydrogen atoms were fixed by HFIX and placed in ideal positions and included in the refinement process using riding model with isotropic thermal parameters. Potential solvent accessible area or void space was calculated using the PLATON multipurpose crystallographic software.

Compound **6** and Compound **8**:

Single crystal X-ray structural studies of **6** and **8** were carried out on a CCD Agilent Technologies (Oxford Diffraction) SUPER NOVA diffractometer. Data for the crystal **6** and **8** were collected at 293(2) K and 150(2) K respectively using graphite-monochromated MoKα radiation (λ= 0.71073 Å). The strategy for the data collection was evaluated by using the CrysAlisPro CCD software. The data were collected by the standard 'phi-omega scan techniques and were scaled and reduced using CrysAlis- Pro RED software. The structures were elucidated by direct methods using SHELXS-97 and refined by full matrix least squares with SHELXL-97, refining on F^2.[31] The positions of all the atoms were obtained by direct methods. All non-hydrogen atoms were refined anisotropically. The remaining hydrogen

View Article Online
DOI: 10.1039/C6DT02969H

atoms were placed in geometrically constrained positions and refined with isotropic temperature factors, generally 1.2Ueq of their parent atoms.

Protein binding experiments:

Protein binding studies of the synthesised compounds were carried out by tryptophan fluorescence quenching experiments using human serum albumin (HSA).The excitation wavelength for HSA was at 280 nm and the quenching of the emission intensity of the tryptophan residues of HSA at 345 nm was monitored using the complexes as quencher with increased concentration. The excitation and emission slit widths and scan rates were kept constant throughout the experiment. A 10 μM stock solution of HSA was prepared using 50 mM tris buffer solution and stored at 4°C for further use. Stock solutions of 5 mM strength were made using synthesized compounds. Fluorometric titration was carried out taking 2 mL of the protein solution and fluorescence intensity was measured as blank. For titration, each time, 10 μL of the stock solution was added to the protein solution and fluorescence intensity was measured. For all the four complexes, up to 100μL of the solution was added to measure fluorescence quenching. The fluorescence quenching data was further analyzed by the Stern–Volmer equation, which again can be expressed in terms of bimolecular quenching rate constant and average life time of the fluorophore as shown in following equation.

$$\frac{F_0}{F} = 1 + Kq\tau_0[Q] = 1 + Ksv[Q]$$

where F_0 and F are the fluorescence intensities in the absence and the presence of a quencher, k_q is the bimolecular quenching rate constant, τ_0 is the average lifetime of fluorophore in the absence of a quencher and [Q] is the concentration of a quencher (metal complexes). K_{SV} is the Stern–Volmer quenching constant in M^{-1}.

Inhibition of Trx-R enzyme:

The inhibition of Trx-R enzyme was carried out using DTNB as substrate according to the protocol given by sigma Aldrich with subsequent modification. Colorimetric assays were

performed with a microplate reader to determine the inhibition of Trx-R. The compound was dissolved to make stock solution in DMSO (5 mM). Mammalian thioredoxin reductase, supplied in 50 mM TrisHCl (pH = 7.4), 10 mM EDTA, 300 mM NaCl and 10% glycerol was diluted 20 times. The reaction mixture in each well consists of working buffer [180 μL; 100 mM potassium phosphate with 10 mM EDTA and 0.24 mM nicotinamide adenine dinucleotide phosphate (NaDPH)], 1X assay buffer (8 μL), TrxR enzymes (2 μL), and positive control (cisplatin) or the ruthenium complex. The reaction mixture were incubated for 15 min at 298 K and then a 100 mM DMSO solution (6 μL) of DTNB was added. Formation of 5-thio-2 nitrobenzoic acid (5-TNB) was monitored with a microplate reader at 412 nm after 15 and 30 min. Non-interference with the assay component was ensured by a negative control experiment with an enzyme free solution. Following equation was used to determine the TrxR enzyme activity.

Unit/mL = [ΔA_{412}/min(TrxR) X dil X vol]/enzvol

ΔA_{412}/min = change in absorbance at 412 nm per minute, ΔA_{412}/min(TrxR) = [ΔA_{412}/min (sample) - ΔA_{412}/min (blank, without enzyme)], dil = sample dilution factor, vol = volume of the reaction and enzvol = volume of the enzyme.

Results and discussion:

Syntheses of complexes

Room temperature substitution of chloride ligand in ruthenium (II) complexes of general formula [Ru(L)(η^6-arene)Cl] (HL^1 = pyridine -2-carboxylic acid(4-nitro-phenyl)-amide, η^6-arene = p-cymene **1** and HL^1 = pyridine -2-carboxylic acid(4-nitro-phenyl)-amide, η^6-arene = benzene **3**, HL^2 = 4-(N-(2-Pyridyl)carbamoyl pyridine , η^6-arene = p-cymene, **5** HL^3 = 3-(N-(2-Pyridyl)carbamoyl) pyridine, η^6-arene = p-cymene **7**) with 1,3,5-triaza-7-phosphoadamantane (PTA) yielded water soluble complexes [Ru(L)(η^6-arene)(PTA)]$^+$ [**2**, **4**, **8**] and [Ru(HL)(η^6-arene)(PTA)]$^{++}$ [**6**] (Scheme 1). Compound **2** and compound **8** were recrystallized in presence of tetrafluoroborate ion in dichloromethane and methanol mixture to generate single crystals of [RuL^1(η^6-p-cymene)PTA]BF_4 **2** and single crystals of [RuL^3(η^6-p-cymene)PTA]BF_4 **8** for solid state characterization whereas single crystals for compound **4** and compound **6** were obtained in presence of NH_4PF_6 as [RuL^1(η^6-benzene)PTA]PF_6 and [Ru(HL^2)(η^6-p-cymene)PTA]$(PF_6)_2$, respectively. All the PTA compounds were as yellow/yellow-orange powders in moderate to good yields (52% - 78%).

Compound [RuL^2(η^6-p-cymene)Cl] **5** and [RuL^3(η^6-p-cymene)Cl] **7** were synthesized by the reaction of N-substituted picolinamide with [Ru(η^6-arene)Cl_2] in an identical method adopted for compound **1** and **3**.

The ^{1}H NMR spectra for complex **2** and **4** display peaks at 8.98 to 7.57 ppm typical for the aromatic ring for ligand L^1. Lack of an NH signal indicates the deprotonation of the ligand. The signals of the arene ring are observed 6.26 to 5.43 ppm and 2.84, 2.28, 0.98 and 0.72 ppm for p-cymene and 6.0 ppm for coordinated benzene ring. The resonance due to the PTA is shifted towards lower field with respect to uncoordinated PTA confirming the coordination. Although usually free PTA shows only two singlets in ^{1}H NMR, however we have observed multiplets when coordinated to metal center as reported earlier.[34] Pyridinyl signals for the ligand HL^2 in compound **5** and **6** are observed in the range 9.03 to 6.81 ppm. Similar peaks in the range of 9.54 to 7.22 were observed for ligand L^3 in compound **7** and **8**. The ^{13}C spectra for compounds **2**, **4**, **6** and **8** also corroborates with the proposed structure. The ^{31}P NMR spectra of compounds **2**, **4** , **6** and **8** show peaks in the range of -30 to -39 ppm as reported earlier.[10] The ESI mass spectra of **2**, **4** , **6**, **8** revealed two main peak envelopes. The higher one corresponds to [RuL(arene)(PTA)]$^+$ and the other being due to [RuL(arene)]$^+$. Compound **5** and **7** produce ESI-MS peak for [RuL(p-cym)]$^+$ moiety.

The solid state structure of the four compounds (**2**, **4**, **6** and **8**) were investigated by X-ray crystallography. All the compounds possess the characteristic psudo-octahedral geometry exhibited by all RAPTA complexes. The η^6 π-bonded arene ring occupying three coordination positions of octahedron, along with two coordination sites occupied by nitrogen donor of N-substituted picolinamide moiety and the other coordination site is occupied by PTA ligand through the phosphorus donor. The asymmetric unit of **2** comprises one complex cation, one BF_4 anion and two water molecules (Fig 1). The $(L^1)^-$ ligand binds the metal in a N,N-chelating fashion, thus giving rise to a five-membered RuNCCN metallacycle, the ruthenium coordination environment being then fulfilled by the P-atom of PTA and by the π-bonded aromatic ring of *p*-cymene. Bond distances and angles are in the range of those found in other ruthenium compounds and PTA or arene derivatives.[14] As a result of steric restrictions, the anionic organic ligand is twisted, as measured by the angle (25.03 º) between the least-square planes of its aromatic and pyridinyl ring; in addition, the least-square planes of the cymene and of the metallacycle rings are

View Article Online
DOI: 10.1039/C6DT02969H

49.84 º apart. The Ru-P bond is nearly orthogonal to the metallacycle (88.95 º), but markedly away from the plane of the arene (130.40 º). The isolated ruthenium complexes form a 1D hydrogen bonded chain along b-axis through C32-H32A...O3 and C34-H34B...O3. The counter BF_4^- anion and two water molecules as solvent of crystallization cemented these parallel chains through further hydrogen bondings [C22-H22...F1, C27-H27B...F1, C12-H12...F1, C30-H30C...F2, C31-H31A...F3, O1S-H1A...F3, C25-H25...F4, C33-H33A...O1S, O2S-H2A...N31] for a 2D hydrogen bonded polymer in *bc*-plane.

Compound **4** also have a similar kind of structure like compound **2 (**Fig 2). However, the twisting in the anionic ligand is much greater here which is found to be 56.3º between the least-square planes of its aromatic and pyridinyl rings. In compound **4** every complex molecule is found to be interacting to three other surrounding molecules through C13-H13...O1, C21-H21...O1, C6-H6...O2, C11-H11...N4, C9-H9...N5. It gives a complicated 3D packing which is further reinforced by octahedral PF_6^- counteranion [C2-H2...F3, H19-H19...F3, C17-H17A...F2 and C22-H22...F1] and one methanol as solvent molecules.

Compound **6** has shown to be crystallizing in monoclinic space group $P2_{1/n}$. Two pyridyl ring in the ligand was found to be twisted at an angle of 37.43° (Fig 3). A methanol molecule is also observed as solvent of crystallization. However the most interesting observation is that the presence of two hexafluorophosphate ion per ruhtenium center indicating the neutral nature of the substituted ligand. A closer observation of the crystal structure reveals comparative shorter C-N bond distance of amino pyridyl fraction of the ligand [C7-N2 1.396(5) Å] along with C8-C9 and C10-C11 bond distance in pyridyl ring [1.365(6) and 1.366(6) Å, respectively) indicating the protonation of the 4-pyridyl nitrogen in presence of ammonium salt during the complexation which leads to essentially change of valence-bond representation of the ligand as per scheme 2. Protonation at 4-pyridyl nitrogen atom gives a partial double bond character to the C7-N2 bond making it a comparatively labile in nature. A similar kind of observation is reported earlier for an alkyl pyridine palladium complex.[35] This subtle change in the system makes the ligand relatively weaker with respect to complex **8** which is evident through comparatively longer bond length between donating nitrogen atom and ruthenium center [N(1)-Ru(1) and N(2)-Ru(2)]. There are two crystallographically independent PF_6- ions present. One of them connect three ruthenium cationic complex through C25-H25A...F1, C23-H23A...F2, C2-H2...F6 and C15-H15...F4. The other PF_6^- connects four such complexes through C27-H27A...F8, C18-H18...F7, C25-H25B...F9, C24-H24A...F12 and C11-H11...F12. The N-pyridyl hydrogen has shown a strong hydrogen bond

with methanol molecule which act as solvent of crystallization through N3-H3N...O111 [1.896 Å]. All these hydrogen bonds leads to formation of 3D-hydrogen bonded network .

Compound **8** crystallized in triclinic space group *C*2/*c*. Two pyridyl ring in the ligand was found to be twisted at an angle of 45.91° (Fig 4). One BF_4^- ion per ruthenium center is observed indicating that the ligand as an uninegative charge unlike compound **6**. This is due to the inability to stabilize the alternative valence bond sturcture as per previous case by the pyridyl N-atom at 3-position. Each BF4- ion is connected to six complex units via hydrogen bond, *viz*. C18-H18...F3, C24-H24B...F3, C26-H26B...F2, C27-H27B...F3, C25-H25B...F1, C19-H19...F1, C1-H1...F1 and C3-H3...F1. Furthermore each molecule is connected to two different molecules through amide O atom via hydrogen bonding [C9-H9...O1, C8-H8...O1, C23-H23B...O1,] and PTA N-atom [C24-H24A...N6]. Altogether it forms a hydrogen bonded 3D network stabilized by counteranion.

Conductivity measurements

In order to investigate the probable structures of compound **6** and **8** in solution, the conductivity of their solution was measured. Conductivity values for compound **6** in acetonitrile and water were found to be 270 Ω^{-1} cm^2 mol^{-1} and 280 Ω^{-1} cm^2 mol^{-1} attesting the 1:2 composition of the complex with retention of the dicationic nature of the ruthenium complex moiety.[36] On the other hand compound **8** is showing molar conductance around 106 Ω^{-1} cm^2 mol^{-1} indicative of 1:1 composition as per solid state crystal structure.[36] The conductance measurement of compound **5** and **7** provide the value corresponding to non-electrolyte which is in agreement with the solid state structure.

Protein Binding Studies:

As a probable candidate of tumour growth inhibition agent we were interested to study the interaction of the synthesized complexes with different biomolecules. However, we did not find any interaction like binding or cleavage to CT-DNA by any of the synthesized complexes. On the other side all the complexes have shown interesting interaction with serum albumin which is important because of its ability to carry active molecules in the blood through their non-covalent conjugation. These are the group of proteins which can bind metal

ions and complexes and transport through blood streams. Fluorescence quenching experiment was carried out to understand the mechanism of action between synthesized complexes and HSA (human serum albumin). The high sensitivity of the tryptophan moiety and its surrounding local environment present in the albumin towards intrinsic fluorescent spectra of proteins can provide certain useful information of structure and dynamics which are often utilized in the study of protein folding and association reaction.

Separate solutions of HSA were titrated against addition of different compounds. In case of HSA binding, addition of reported compounds to the respective protein solution causes significant decrease of initial fluorescence intensity for the compounds number **2**, **4, 6, 8** respectively. In case of compound no. **2** and **4**, plots [F_0/F vs [Q]] with upward curvature towards y-axis. were obtained, signifying concurrent quenching by collision as well as by complex formation with the same quencher.[37]To get further insight in the quenching process, the fluorescence quenching data were analyzed with Stern-Volmer equation as described in experimental section. The value of K_{SV} obtained by linear plot of F_0/F vs [Q] follows the order **2** > **4** > **8** > **6**. The nitro substituted ligand based complexes (**2** and **4**) are capable of quenching the tryptophan fluorescence more strongly with respect to pyridyl ligand based complexes (**6** and **8**). This may be due to the presence of substituted phenyl ring instead of pyridyl group which may lead to stronger hydrophobic interaction with the protein. Similarly p-cymene complex **2** has been found to be more interactive with protein due to enhanced hydrophobic interaction of methyl and isopropyl groups of p-cymene with tryptophan site.[38] The k_q value obtained for all the complexes are found to be in the range of 8.04 X 10^{11} - 6.41 X 10^{13} L mol^{-1} S^{-1}, indicating the involvement of static quenching mechanism.[39] To determine the binding constant and number of binding sites, the Scatchard equation was employed, which is given by

$$log \frac{[F0-F]}{F} = \log Ka + n \ \log[Q]$$

Where K_a and n are the binding constant and number of binding sites respectively, and F_0 and F are the fluorescence intensities in the absence and presence of the quencher respectively. Thus, a plot of log $[(F_0 - F)/F]$ versus log[Q] can be used to determine the value of binding constant (from the intercept) and number of binding sites (from the slope). Using Scatchard plot, binding constants and n values were also calculated for all the compounds which are

represented in table 2. The value of n for all the complexes are in the range ~1, indicating comparable binding property of the complexes with HSA.

Growth Inhibition of ruthenium-arene complexes:

The antiproliferative activities of compound **2, 4, 6,** and **8** were studied against three cell lines *viz*. breast cancer cell line MCF 7, ovarian carcinoma cell line A2780 and lungs cancer cell line A549. SRB assay is utilized to obtain the results in terms of GI_{50} (concentration of drug that produces 50% inhibition of the cells), TGI (concentration of the drug that produces total inhibition of the cells) and LC_{50} (concentration of the drug that kills 50% of the cells). All cancer cells were exposed to 24h to increasing concentrations of the compounds, and their proliferation were determined. Adriamycin, a chemotherapeutic drug was used as a positive control. Though compound **2**, **4** and **8** do not show much cell growth inhibition, however quite interestingly compound **6** have shown remarkable cell growth inhibition properties against all cell lines almost to the tune of adriamycin in terms of molar concentration. All the data are summarized in table 3 and in fig 5.

Stability study of compound 6 and 8:

To understand what might leading compound **6** to be so active against cancer cell lines whereas similar compound **8** is non active, we have performed the solution stability study of complex **6** and **8**. Many a times cleavage of M-L bond is found to be the first step for the activation of Ru-complexes in solution.[40] Thus it is of considerable interest to know the nature of species generated in solution which is responsible for its cytotoxic behaviour. Thus, the hydrolytic behaviour of the compound **6** was studied to check its stability under pseudopharmacological conditions. The decomposition nature of the compound was studied in 5 mM NaCl solution (corresponding to the low intracellular NaCl concentration in cells) and in 100 mM NaCl solution (assuming to the higher NaCl levels in blood plasma). Compound **6** was dissolved in aqueous NaCl (c= 5 or 100 mM in D_2O containing 10% D6-DMSO) and maintained at 37°C for 7 days. Decomposition of the compound was monitored using ^{31}P NMR spectroscopy. Compound **6** underwent immediate transformation in both the solutions (5 mM and 100 mM NaCl) with the substitution of picolinamide ligand with two chloride ions to form $[Ru(cym)(PTA)Cl_2]$ which is evident by the typical ^{31}P singlet peak at -35.5 ppm (Fig 6 and Fig 7),[41] whereas no peak, corresponding to the starting complex **6** at -

38.9 ppm was observed any more. Analysing the ^{31}P NMR data, it can be said that compound **6** is unstable in intracellular NaCl concentration in cells as well as in extracellular blood plasma. It undergoes instant transformation to form RAPTA-C predominantly. However, a similar study with complex **8** has shown the compound is quite stable at both 5 mM and 100 mM concentration of NaCl without showing any other ^{31}P peak even after 7 days except that characteristic one for complex **8** itself at -37.8 ppm (Fig 8 and Fig 9). This results are in agreement with the observation of solid state structure determination where a valence bond tautomer of ligand HL^2 gets stabilized making the substituted picolinamide ligand weaker one with respect to ligand HL^3 in complex **8**. Perhaps this dissociation of the ligand is playing some important role in the observed antiproliferative property of complex **6**.

As complex **6** has shown tendency to form $[Ru(cym)(PTA)Cl_2]$ in NaCl solution therefore to check the possibility that if $[Ru(cym)(PTA)Cl_2]$ is the actual active species for antiproliferative properties of complex **6**, we have performed cytotoxicity study of $[Ru(cym)(PTA)Cl_2]$ against all three cancer cell lines. It has been observed that that GI_{50} values for $[Ru(cym)(PTA)Cl_2]$ is quite high against all the three cell lines (table 5). Thus, it can be concluded that $[Ru(cym)(PTA)Cl_2]$ is not the responsible entity for the antiproliferative activity of compound **6**. In physiological medium, after the ligand gets liberated from the coordination sphere owing to its labile nature, some other biomolecule like thioredoxin reductase; which is already present in the physiological medium might get attached to ruthenium centre which activates the compound to act as an antiproliferative agent.

Mammalian Trx-R Inhibition:

To further investigate the possible pathway by which compound **6** is showing growth inhibition properties we have carried out mammalian thioredoxin reductase inhibition properties of the synthesized complexes. Mammalian thioredoxin reductases (TrxR) are large homodimeric proteins that play an important role in the intracellular redox metabolism, along with a few other biochemical systems.[23] Thioredoxin reductases are characterized by broad substrate specificity and by easily accessible redox centers. In mammalian TrxR, the redox center consists of a cysteine selenocysteine redox pair that approaches the N-terminal active site of the other subunit for electron transfer.[42] The active site selenolate group, after reduction, manifests a large propensity to react with “soft” metal ions, making TrxR a likely pharmacological target for a vast array of metallodrugs. This is probably the reason why various gold(I) and platinum(II) compounds were earlier reported to be potent inhibitors of

mammalian thioredoxin reductase.[43,44] Recent studies suggest that some ruthenium complexes also show Trx-R inhibition owing to its 'soft' nature.[42,45] Complexes **2**, **4**, **6** and **8** have been tested for TrxR inhibition at various concentration. Whereas compound **2**, **4** and **8** have shown very little activity towards Trx-R, compound **6** was found highly active against the enzyme. The IC_{50} value was found to be 11.07μM which might be due to the weakly bound substituted picolinamide ligand which dissociates easily in presence of thioredoxin reductase with selenocysteine redox center. The selenocysteine group might get coordinated to ruthenium center inducing inhibition of the enzyme which might be a plausible reason of inherent tumor growth inhibition property of compound **6**.

Conclusion:

Four new ruthenium (II) complexes containing N-substituted picolinamide ligand with amphiphilic PTA ligands have been synthesized and characterised. All the complexes are water soluble and their interaction with HSA protein molecules have been explored. Cytotoxicities for the prepared compounds have been evaluated for different cell lines. Compound **2**, **4** and **8** are having general molecular formula [RuL(η^6-arene)(PTA)]X where the ligands (L) behave as monoanionic ligand. Whereas in compound **6** the ligand takes a valence bond tautomerised protonated form which behaves as neutral polar ligand making the complex dicationic in nature. Interestingly among the four compounds, compound **6** show very promising antiproliferative activity against all the three cell lines with GI_{50} value comparative to adrimycin, a cytotoxic drug in μM scale. To understand the mechanistic pathway, protein binding studies, hydrolysis and ligand substitution and mammalian Trx-R inhibition studies were carried out for all the complexes. Though all the compounds show significant binding with HSA protein, whereas, only compound **6** strongly inhibits Trx-R activity which is probably having some correlation with its strong antiproliferative property.

Supporting Information :

CCDC 1036656, 1449639, 1477542 and 1444481 contain the supplementary crystallographic data for **2**, **4, 6** and **8** respectively. These data can be obtained free of charge via http://www.ccdc.cam.ac.uk/conts/retrieving.html, or from the Cambridge Crystallographic Data Centre, 12 Union Road, Cambridge CB2 1EZ, UK; fax: (+44) 1223-336-033; or e-mail: deposit@ccdc.cam.ac.uk.

View Article Online
DOI: 10.1039/C6DT02969H

Acknowledgement :

We are grateful for the financial support received from SERB, DST Govt of India through research grant no **SR/S1/IC-43/2012**. We are also thankful to the Sophisticated Instrument Center, IIT Indore for the structure elucidation (Compound **6** and **8**).

View Article Online
DOI: 10.1039/C6DT02969H

Schemes:

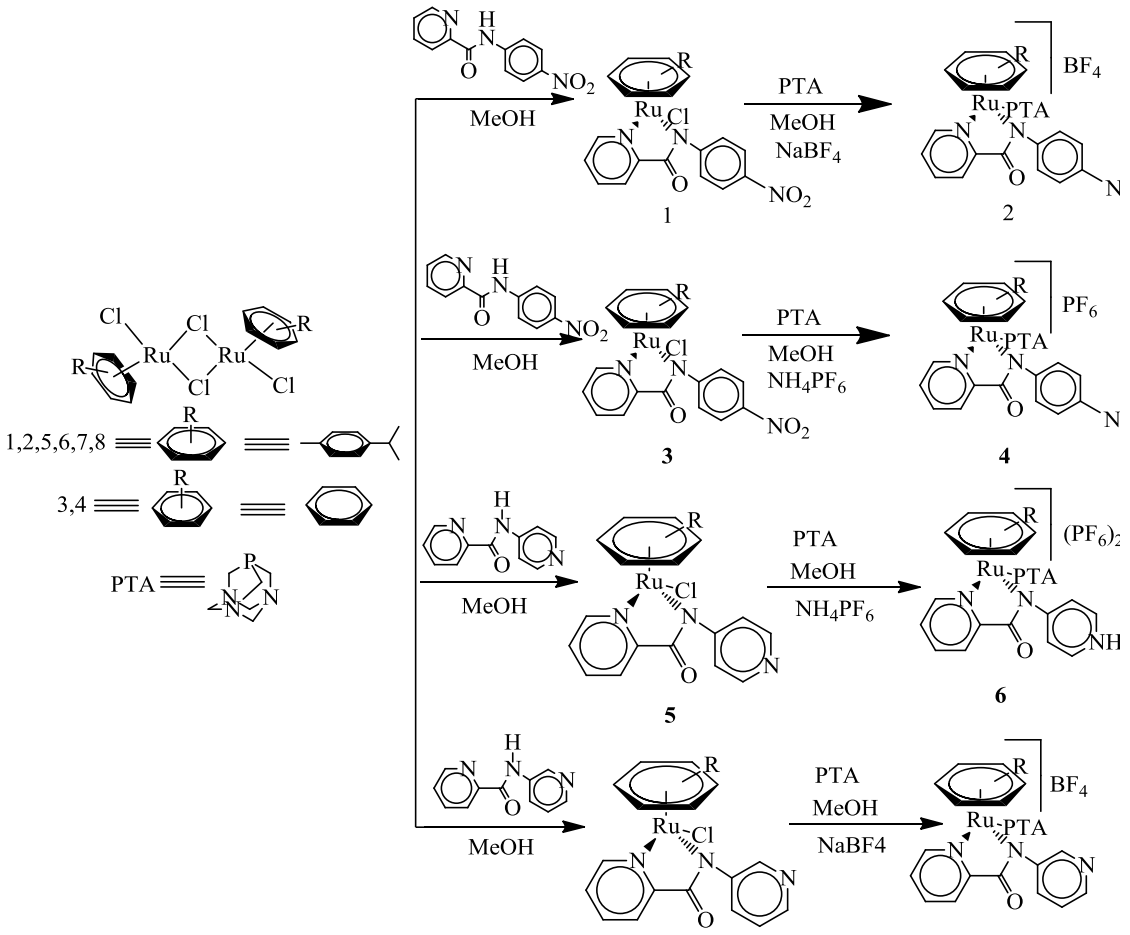

Scheme 1: Synthesis of compounds **[Ru(L^1)(η^6-p-cymene)PTA][BF$_4$] 2**, **[Ru(L^1)(η^6-benzene)PTA][PF$_6$] 4**, **[Ru(HL^2)(η^6-p-cymene)PTA][PF$_6$]$_2$ 6**, and **[Ru(L^3)(η^6-p-cymene)PTA][BF$_4$] 8**

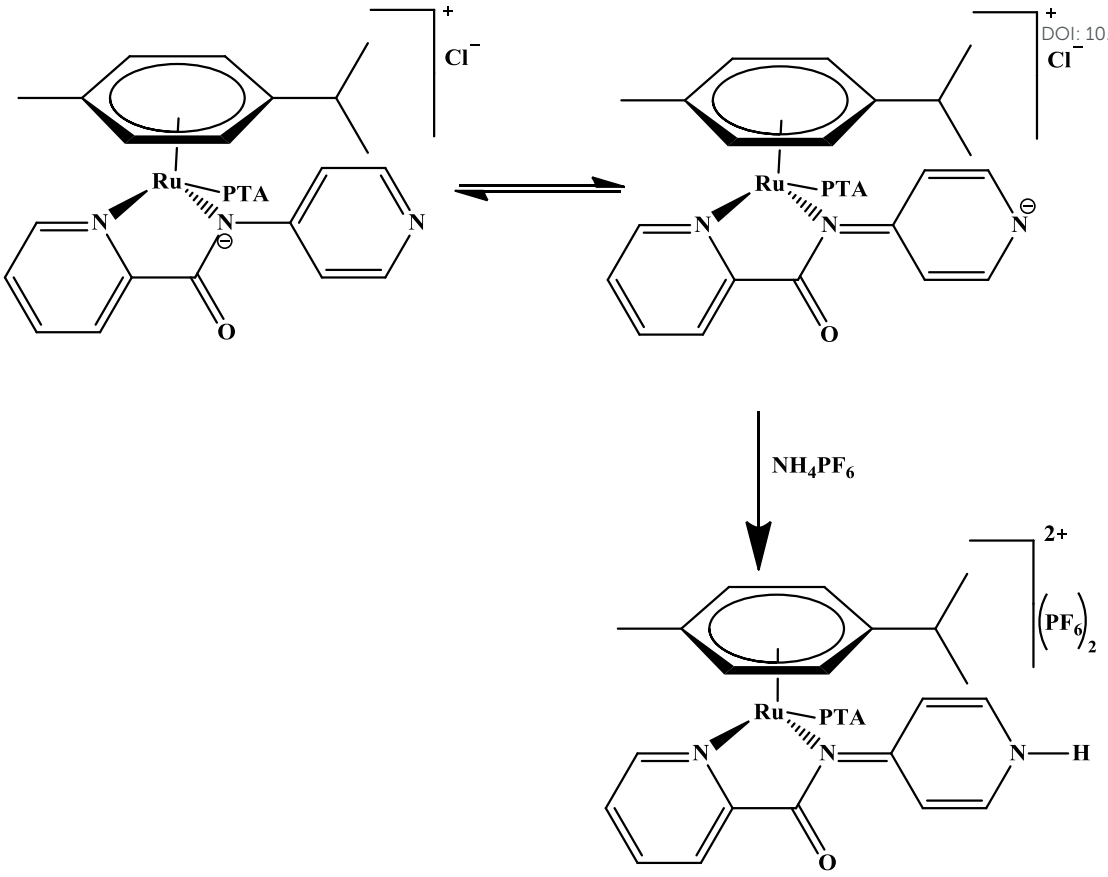

Scheme 2: Valence bond tautomerism of compound **6**

Figures:

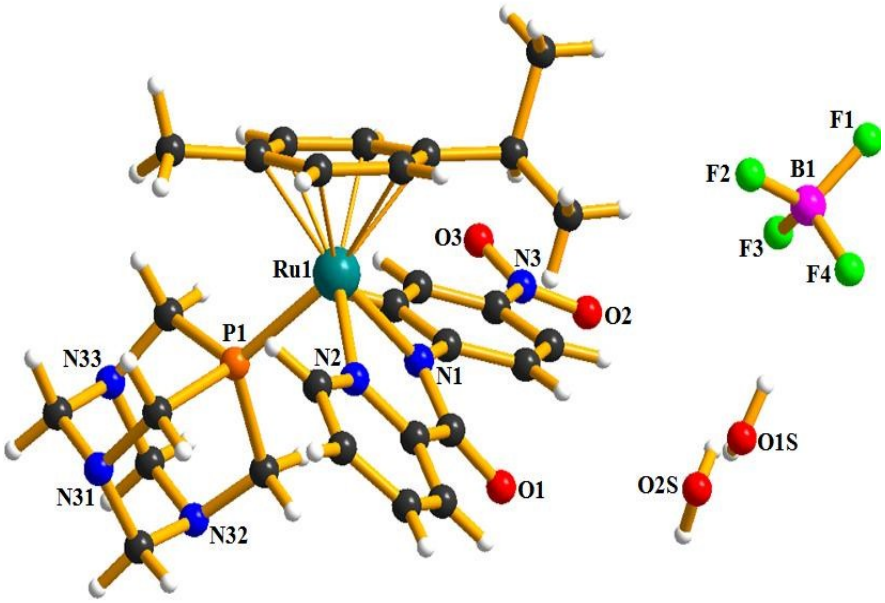

Fig 1: The solid state crystal structure of compound **2** with partial atomic numbering scheme

View Article Online
DOI: 10.1039/C6DT02969H

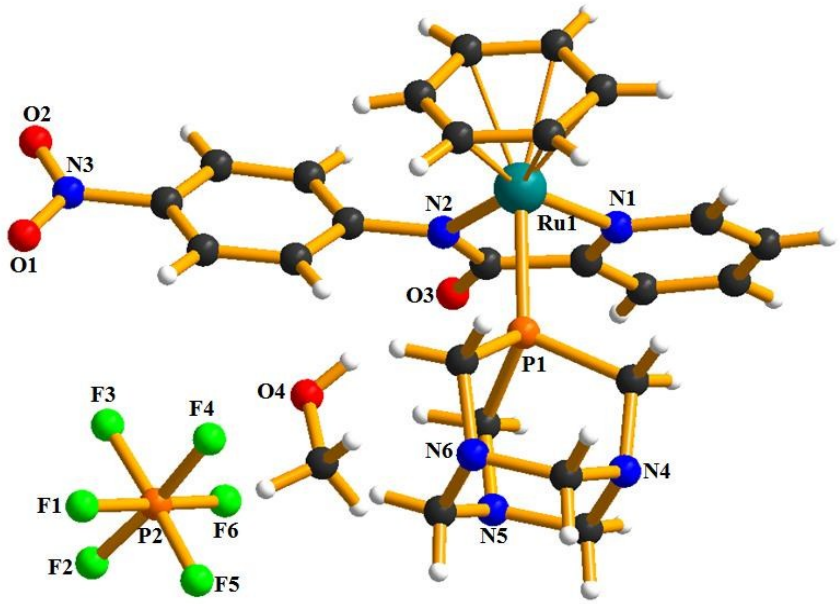

Fig 2: The solid state crystal structure of compound **4** with partial atomic numbering scheme

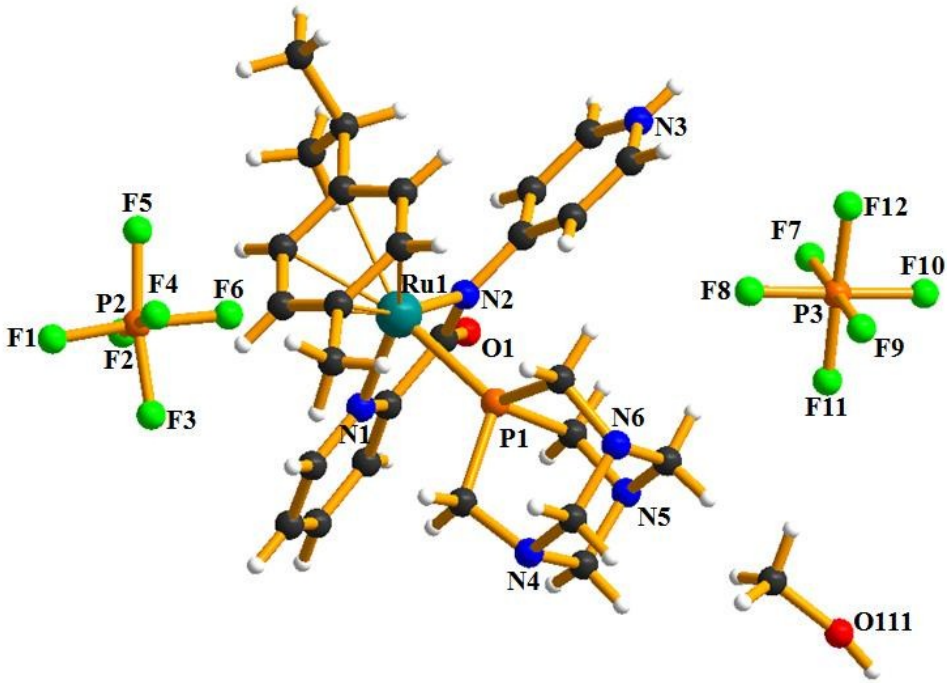

Fig 3: The solid state crystal structure of compound **6** with partial atomic numbering scheme

View Article Online
DOI: 10.1039/C6DT02969H

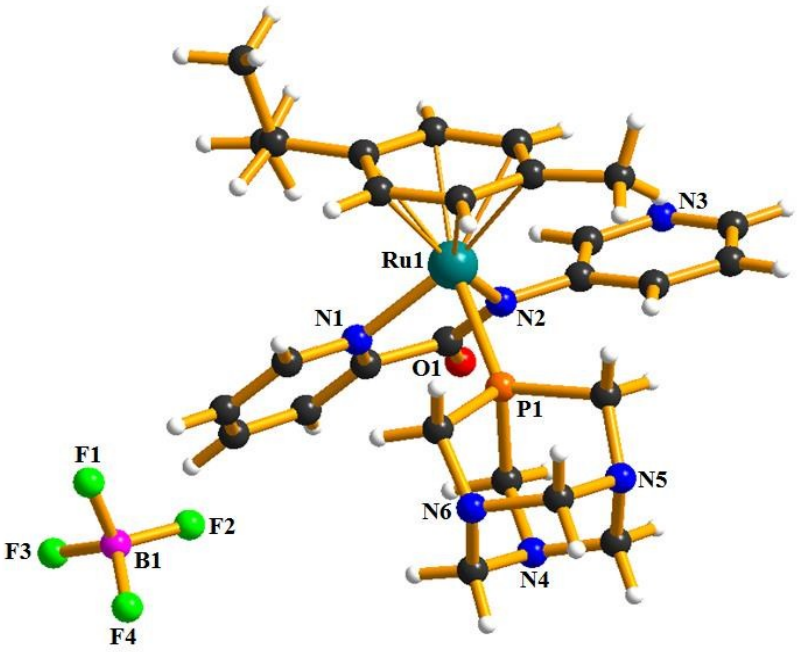

Fig 4: The solid state crystal structure of compound **8** with partial atomic numbering scheme

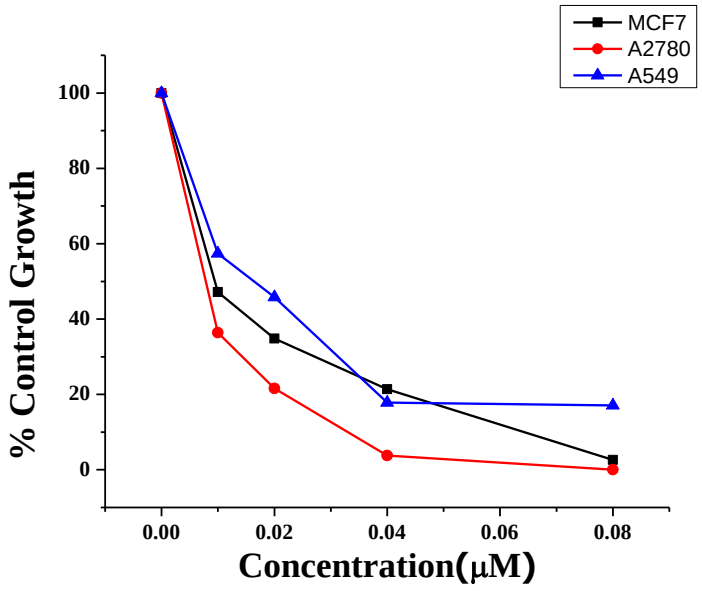

Fig 9: analysis of GI_{50} value of Compound **6** against different cell lines using adriamycin as positive control

View Article Online
DOI: 10.1039/C6DT02969H

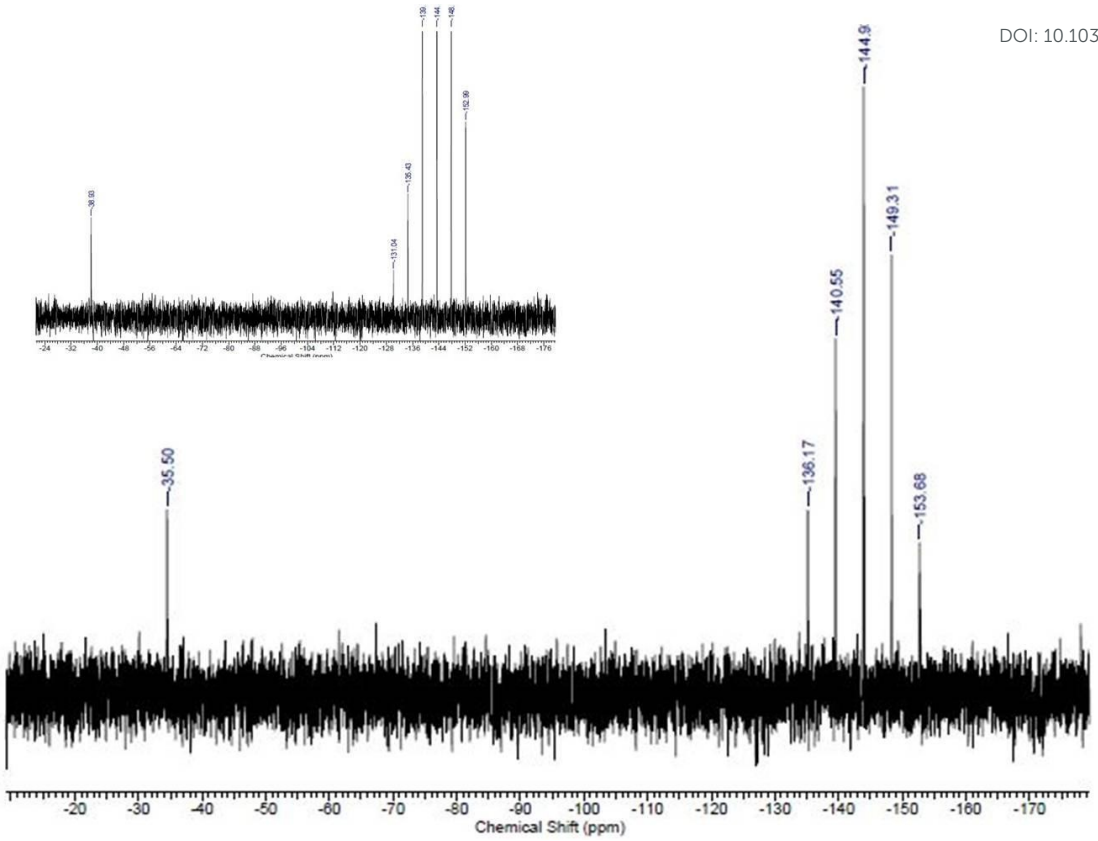

Fig 6: ^{31}P NMR of compound **6** in 5mM NaCl solution after 7 days. ^{31}P NMR of compound **6** in 10% D6-DMSO [inset].

View Article Online
DOI: 10.1039/C6DT02969H

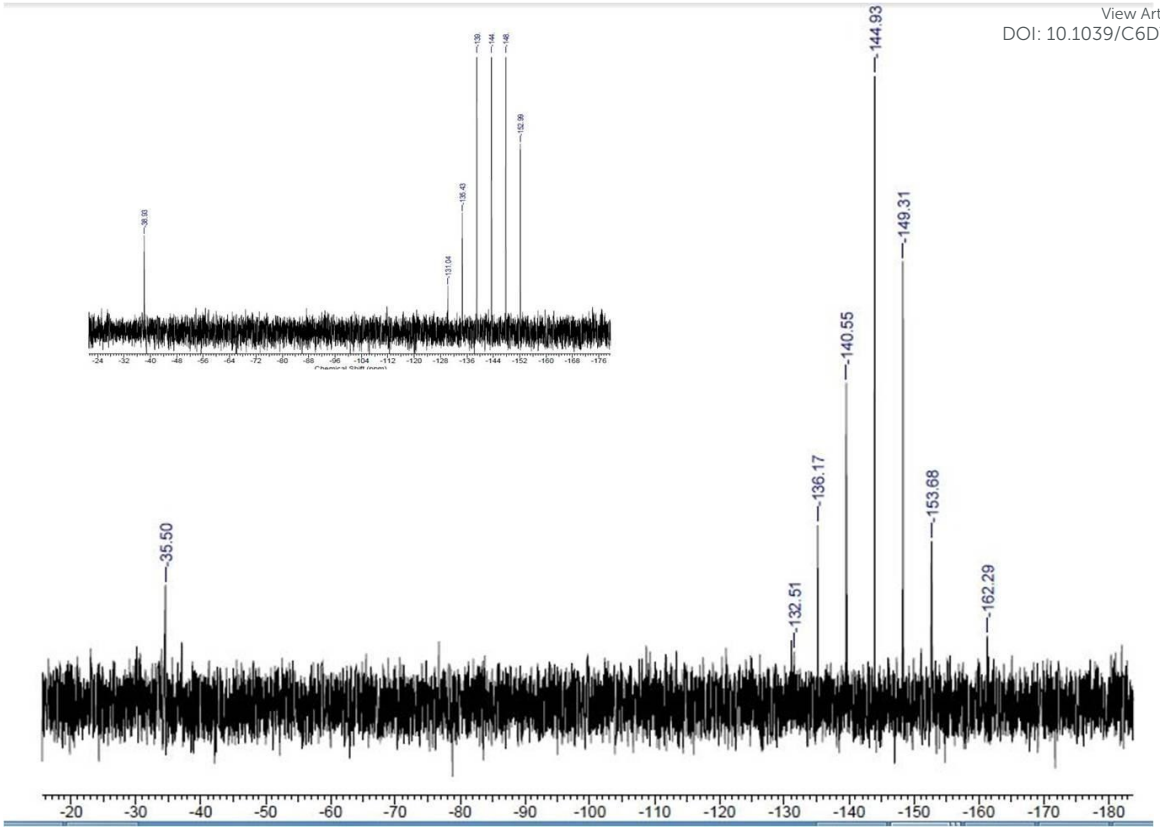

Fig 7: ^{31}P NMR of compound **6** in 100mM NaCl solution after 7 days. ^{31}P NMR of compound **6** in 10% D6-DMSO [inset].

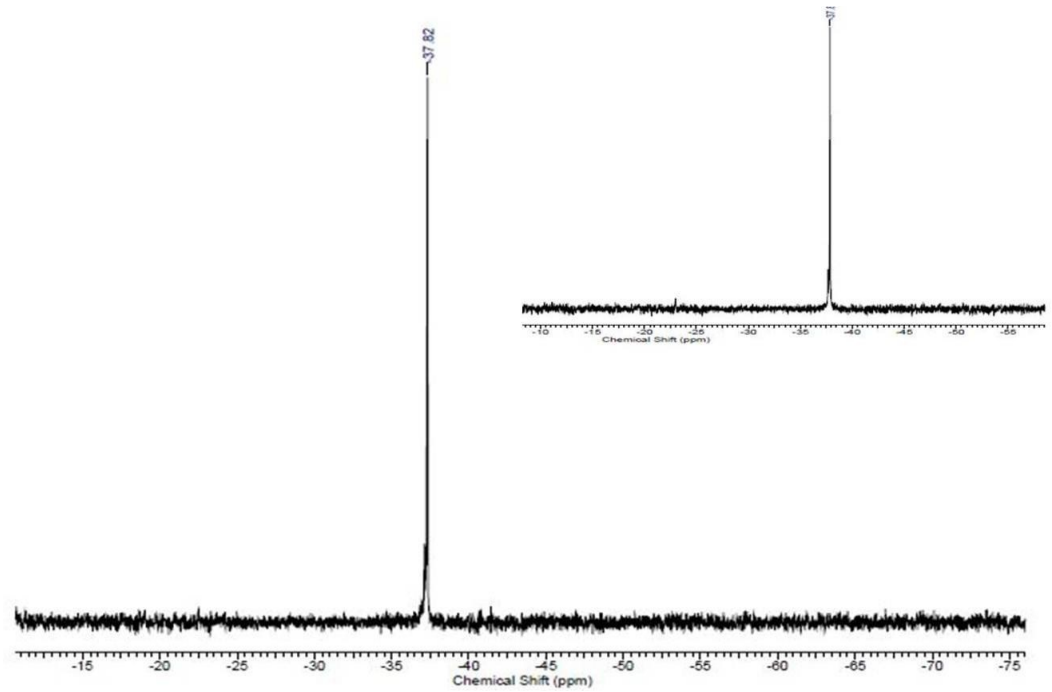

Fig 8: ^{31}P NMR of compound **8** in 5 mM NaCl solution after 7 days. ^{31}P NMR of compound **8** in 10% D6-DMSO [inset].

View Article Online
DOI: 10.1039/C6DT02969H

Fig 9: ^{31}P NMR of compound **8** in 100mM NaCl solution after 7 days. ^{31}P NMR of compound **8** in 10% D6-DMSO [inset].

View Article Online
DOI: 10.1039/C6DT02969H

Tables:

Table 1: Summary of the Crystallographic data for complexes **2**, **4**, **6**, **8**

	2	**4**	**6**	**8**
formula	$[C_{28}H_{34}N_6O_3PRu][BF_4].2(H_2O)$	$[C_{24}H_{26}N_6O_3PRu][PF_6].(CH_3OH)$	$[C_{27}H_{35}N_6OPRu]2[PF_6].(CH_4O)$	$[C_{27}H_{34}N_6OPRu]BF_4$
Formula wt	757.49	755.52	913.63	677.45
Crys syst	Triclinic	Triclinic	Monoclinic	Monoclinic
space group	P -1	P-1	P 21/n	C 2/c
a(Å)	9.2108(7)	10.219(5)	8.9084(2)	39.549(2)
b (Å)	10.1314(8)	10.410(5)	35.5854(8)	12.8897(4)
c (Å)	18.1559(12)	15.762(5)	11.1155(3)	12.5616(3)
α (deg)	105.174(3)	76.497(5)	90	90
β (deg)	98.350(3)	79.789(5)	96.018(2)	90.442(3)
γ (deg)	92.197(3)	63.638(5)	90	90
V ($Å^3$)	1612.69	1455.6(11)	3504.29(15)	6403.4(4)
Z, molecules/cell	2	2	4	8
Density(g/cm^3)	1.560	1.724	1.732	1.405
Absorp coeff (mm^{-1})	0.606	0.731	0.687	0.593
λ [Mo-Kα] (Å)	0.71073	0.71073	0.71073	0.71073
T(K)	150	293	293(2)	150(2)

no of reflns collected	43759	68017	52669	25101
No of independent reflns	5967	7243	11685	5639
No of obsd reflns	5626	6673	8373	4828
R1	0.0348	0.0419	0.0607	0.0458
wR2	0.0854	0.1422	0.1717	0.1222
GOF	1.052	1.04	1.119	1.133

Table 2: Selected Bond Lengths (Å) for Compounds **2**, **4**, **6** and **8**

Compound	Ru(1)-P(1)	Ru(1)-N(1)	Ru(1)-N(2)	Ru(1)-$C_{centroid}$
2	2.3112(7)	2.118(2)	2.072(2)	1.735
4	2.327(1)	2.092(3)	2.096(3)	1.735
6	2.319(1)	2.086(3)	2.115(3)	1.736
8	2.319(1)	2.079(3)	2.100(3)	1.736

View Article Online
DOI: 10.1039/C6DT02969H

Table 3: Selected Bond Angles (°) for Compounds **2**, **4**, **6** and **8**

Compound	P(1)-Ru(1)-N(1)	P(1)-Ru(1)-N(2)	N(1)-Ru(1)-N(2)
2	87.54(7)	86.90(7)	77.80(9)
4	87.37(8)	88.84(8)	76.9(1)
6	85.14(9)	89.38(9)	77.9(1)
8	83.70(9)	90.30(8)	77.2(1)

Table 4: Various parameters obtained from HSA interaction with the prepared compounds

HSA	$K_{sv}(M^{-1})$	$Kq(M^{-1}S^{-1})$	$Ka(M^{-1})$	n
Compound **2**	$3.21x10^{4}$	$5.19x10^{12}$	$2.24x10^{5}$	1.23
Compound **4**	$2.87x10^{4}$	$4.64x10^{12}$	$1.14x10^{7}$	1.55
Compound **6**	$4.97x10^{3}$	$8.04x10^{11}$	$1.41x10^{4}$	1.09
Compound **8**	$5.60x10^{3}$	$8.28x10^{11}$	$4.87x10^{4}$	1.24

Table 5: GI_{50} value (μM) of the prepared compounds in human cancer cells

Compound	MCF7	A2780	A549
2	>80	>80	>80
4	>80	>80	>80
6	<0.1	<0.1	<0.1
8	>80	>80	>80
$[Ru(cym)(PTA)Cl_2]$	>80	>80	>80
Adriamycin	<0.1	<0.1	<0.1

View Article Online
DOI: 10.1039/C6DT02969H

Reference:

1. A. K. Singh, D. S. Pandey, Q. Xu, P. Braunstein, *Coord. Chem. Rev.*, 2014, **270-271**, 31.

2. C. G. Hartinger, P. J. Dyson, *Chem. Soc. Rev.*, 2009, **38**, 391.

3. J. Furrer, S. G. Fink, *Coord. Chem. Rev.*, 2016, **309**, 36.

4. B. Therrin, *CrystEngComm*., 2015, **17**, 484.

5. H. K. Liu, P. J. Sadler, *Acc. Chem. Res.*, 2011, **44**, 349.

6. Y. K. Yan, M. Melchart, A. Habtemariam, P. J. Sadler, *Chem.Commun.*, 2005, 4764.

7. A. Habtemariam, M. Melchart, R. Ferna´ndez, S. Parsons, D. H. I. Oswald, A. Parkin, P. A. F. Fabbiani, E. J. Davidson, A. Dawson, E. H. Aird, I. D. Jodrell, P. J. Sadler, *J. Med. Chem.*, 2007, **49**, 6858.

8. A. Kurzwernhart, W. Kandioller, C. Bartel, S. Bächler, R. Trondl, G. Mühlgassner, M. A. Jakupec, V. B. Arion, D. Marko, B. K. Keppler, C.G. Hartinger, *Chem.Commun.*, 2012, 4839.

9. W. Guo, W. Zheng, Q. Luo, X. Li, Y. Zhao, S. Xiong, F. Wang, *Inorg. Chem.*, 2013, **52**, 5328.

10. R. Pettinari, F. Marchetti, F. Condello, C. Pettinari, G. Lupidi, R. Scopelliti, S. Mukhopadhyay, T. Riedel, P. J. Dyson, *Organometallics*, 2014, **33**, 3709.

11. R. Pettinari, C. Pettinari, F. Marchetti, B. W. Skelton, A. H. White, L. Bonfili, M. Cuccioloni, M. Mozzicafreddo, V. Cecarini, M. Angeletti, M. Nabissi, A. M. Eleuteri, *J. Med. Chem.*, 2014, **57**, 4532.

12. K. J. Kilpin, S. M. Cammack, C. M. Clavel, P.J. Dyson, *Dalton Trans.*, 2013, **42**, 2008.

13. K. J. Kilpin, C. M. Clavel, F. Edafe, P. J. Dyson, *Organometallics*, 2012, **31**, 7031.

14. C. A. Vock, A. K. Renfrew, R. Scopelliti, L. Juillerat-Jeanneret, P. J. Dyson, *Eur. J. Inorg. Chem.*, 2008, 1661.

15. W. H. Ang, E. Daldini, C. Scolaro, R. Scopelliti, L. Juillerat- Jeannerat, P. J. Dyson, *Inorg. Chem,*. 2006, **45**, 9006.

16. C. K. Vock, A. K. Renfrew, R. Scopelliti, L. Juillerat-Jeanneret, P. J. Dyson, *Eur. J. Inorg. Chem.*, 2008, 1661.

17. P. Govender, L. C. Sudding, M. C. Clavel, P. J. Dyson, B. Therrien, G. S. Smith, *Dalton Trans.*, 2013, **42**, 1267.

18. Z. Almodares, S. J. Lucas, B.D. Crossley, A. D. Basri, C. M. Pask, A. J. Hebden, R. M. Phillips, P.C. McGowan, *Inorg. Chem.* 2014, **53**, 727.

19. S. J. Lucas, R. M. Lord, R. L. Wilson, R. M. Phillips, V. Sridharan, P. C. McGowan, *Dalton Trans.*, 2012, **41**, 13800.

20. S. H. van Rijt, A. J. Hebden, T. Amaresekera, R. J. Deeth, G. J. Clarkson, S. Parsons, P. C. McGowan, P. J. Sadler, *J. Med. Chem.*, 2009, **52**, 7753.

21. S. Mokesch, M. S. Novak, A. Roller, M. A. Jakupec, W. Kandioller, B. K. Keppler, *Organometallics*, 2015, **34**, 848.

22. P. J. Dyson, G. Sava, *Dalton Trans.*, 2006, 1929.

23. A. Casini, C. Gabbiani, F. Sorrentino, M. P. Rigobello, A. Bindoli, T. J. Geldbach, A. Marrone, N. Re, C. G. Hartinger, P. J. Dyson, L. Messori, *J. Med. Chem.*, 2008, **51**, 6773.

24. K. D. Camm, A. El-Sokkary, A. L. Gott, P. G. Stockley, T. Belyaeva, P. C. McGowan, *Dalton Trans.*, 2009, 10914.

25. R. Li, M. P. Martin, Y. Liu, B. Wang, A. R. Patel, J. Zhu, N. Sun, R. Pireddu, N. J. Lawrence, J. Li, E. B. Haura, S. Sung, W. C. Guida, E. Schonbrunn, M. S. Sebti, *J. Med. Chem.*, 2012, **55**, 2474.

26. N. J. M. Sanghamitra, M. K. Adwankar, A. S. Juvekar, V. Khurajjam, C. Wycliff, A. G. Samuelson, *Indian J. Chem. Sect. A*, 2011, **50**, 465.

27. SMART & SAINT Software Reference manuals, version 5.0, Bruker AXS Inc., Madison, WI, 1998

28. SAINT, Area Detector Integration Software; Siemens Analytical Instruments Inc.: Madison, WI, USA, 1995.

29. G. M. Sheldrick, SADABS, Program for Semi-empirical Absorption Correction; University of Göttingen: Göttingen, Germany, 1997.

30. G. M. Sheldrick, T. R. Schneider, [16] SHELXL: Highresolution refinement. In Methods in Enzymoogy; Carter, C. W., Jr., Ed.; Academic Press: New York, 1997; Vol. 276, pp 307-326

31. G. M. Sheldrick, *Acta Crystallogr., Sect. A: Found. Crystallogr.* 2008, **A64**, 112.

32. L. J. Farrugia, *J. Appl. Crystallogr.*, 1999, **32**, 837.

33. A. J. Spek, *Appl. Crystallogr.*, 2003, **36**, 7.

34. S. Seršen, J. Kljun, K. Kryeziu, R. Panchuk, B. Alte, W. Körner, P. Heffeter, W. Berger, I.Turel, *J. Med. Chem.*, 2015, **58**, 3984.

35. P. D. W. Boyd, L. J. Wright, M. N. Zafar, *Inorg. Chem.*, 2011, **50**, 10522.

36. I. Ali, A. W. Wani, K. Saleem, *Synthesis and Reactivity in Inorganic, Metal-Organic, and Nano-Metal Chemistry*, 2013, **43:9**, 1162.

37. M. Alagesan, S. P. Nattamai, Bhuvanesh, N. Dharmaraj, *Dalton Trans.*, 2014, **43**, 6087.

38. M. Ganeshpandian, R. Loganathan, E. Suresh, A. Riyasdeen, M. A. Akbarshad, M. Palaniandavar, *Dalton Trans.*, 2014, **43**, 1203.

39. M. Das, R. Nasani, M. Saha, S. M. Mobin, S. Mukhopadhyay, *Dalton Trans.*, 2015, **44**, 2299.

40. R. Mitra, A. G. Samuelson, *Eur. J. Inorg. Chem.*, 2014, **22**, 3536.

41. C. Scolaro, C. G. Hartinger, C. S. Allardyce, B. K. Keppler, P. J. Dyson, *J. Inorg. Biochem.*, 2008, **102**, 1743.

42. P. Mura, M. Camalli, A. Bindoli, F. Sorrentino, A. Casini, C. Gabbiani, M. Corsini, P. Zanello, M. P. Rigobello, L. Messori, *J. Med. Chem.*, 2007, **50**, 5871.

43. M. Coronnello, E. Mini, B. Caciagli, M. A. Cinellu, A. Bindoli, C. Gabbiani, L. Messori, *J. Med. Chem.*, 2005**, 48**, 6761.

44. C. Marzano, V. Gandin, A. Folda, G. Scutari, A. Bindoli, M. P. Rigobello, *Free Radical Biol. Med.*, 2007, 872.

45. A. Casini, C. Gabbiani, F. Sorrentino, M. P. Rigobello, A. Bindoli, T. J. Geldbach, A. Marrone, N. Re, C. G. Hartinger, P. J. Dyson, L. Messori, *J. Med. Chem.*, 2008**, 51**, 6773.